TABLE S1. Patient characteristics and baseline results

Parameters	
Recipient sex	male
Underlying renal disease	IgA nephropathy
Prior kidney transplant (deceased donor)	December, 1992
Variables recorded - second kidney transplantation	
Deceased donor transplantation	March 2005
Recipient age at transplantation	36 years
Donor age	56 years
HLA mismatch (A, B, DR)	2-1-1
Current cytotoxic panel reactivity	4%
Virtual panel reactivity[a]	94%
Preformed DSA[a]	
HLA class I specificities	A*24:02, A*02:01
HLA class II specificities	DRB1*15:01; DRB3*01:01; DRB5*01:01; DQB1*06:02
Immunodominant DSA, specificity (MFI)	DQB1*06:02 (15.802)
Initial immunosuppression	Basiliximab induction, sirolimus, MPS, steroids
Early rejection episode	7 days post-Tx (DGF); biopsy: Banff II rejection (Banff 97)[b]; response to ATG
Variables recorded at the time of ABMR diagnosis	
Time of ABMR diagnosis	13 years after transplantation (June, 2018)
eGFR (MDRD equation)	27.7 ml/min/1.73 m^2
Protein/creatinine ratio	2730 mg/g
DSA specificity (MFI)	DQB1*06:02 (3761)
Morphologic rejection phenotype	C4d-negative chronic active ABMR (no TCMR)
Acute lesion scores	g2, ptc1, t0, i0, v0
Chronic lesion scores	cg3, ci1, ct0, cv1
Molecular rejection phenotype (MMDx)	Fully developed ABMR (archetypal analysis)
ABMR score	0.79
All rejection score	0.68

ABMR, antibody-mediated rejection; ATG, anti-thymocyte globulin; cg, glomerular basement membrane double contours; ci, interstitial fibrosis; ct, tubular atrophy; cv, vascular fibrous intimal thickening; DGF, delayed graft function; DSA, donor-specific antibody; g, glomerulitis; i, interstitial inflammation; MFI, mean fluorescence intensity; MDRD, Modification of Diet in Renal Disease; MPS, mycophenolic acid; TCMR, T cell-mediated rejection; t, tubulitis; Tx, transplantation; v, intimal arteritis

[a]Single antigen testing was performed retrospectively on a biobanked pretransplant serum. Virtual panel reactive antibodies were calculated according to the Eurotransplant virtual PRA calculator (etrl.org/Virtual PRA).

[b]Re-evaluation of this indication biopsy revealed an isolated v lesion (v1) with microcirculation inflammation (g2, ptc2), but without tubulo-interstitial infiltrates (t0, ti0, i0), glomerular double contours (cg0) or IFTA. According to the updated Banff scheme, the specimen was reclassified as C4d-negative active ABMR.

Figure S1

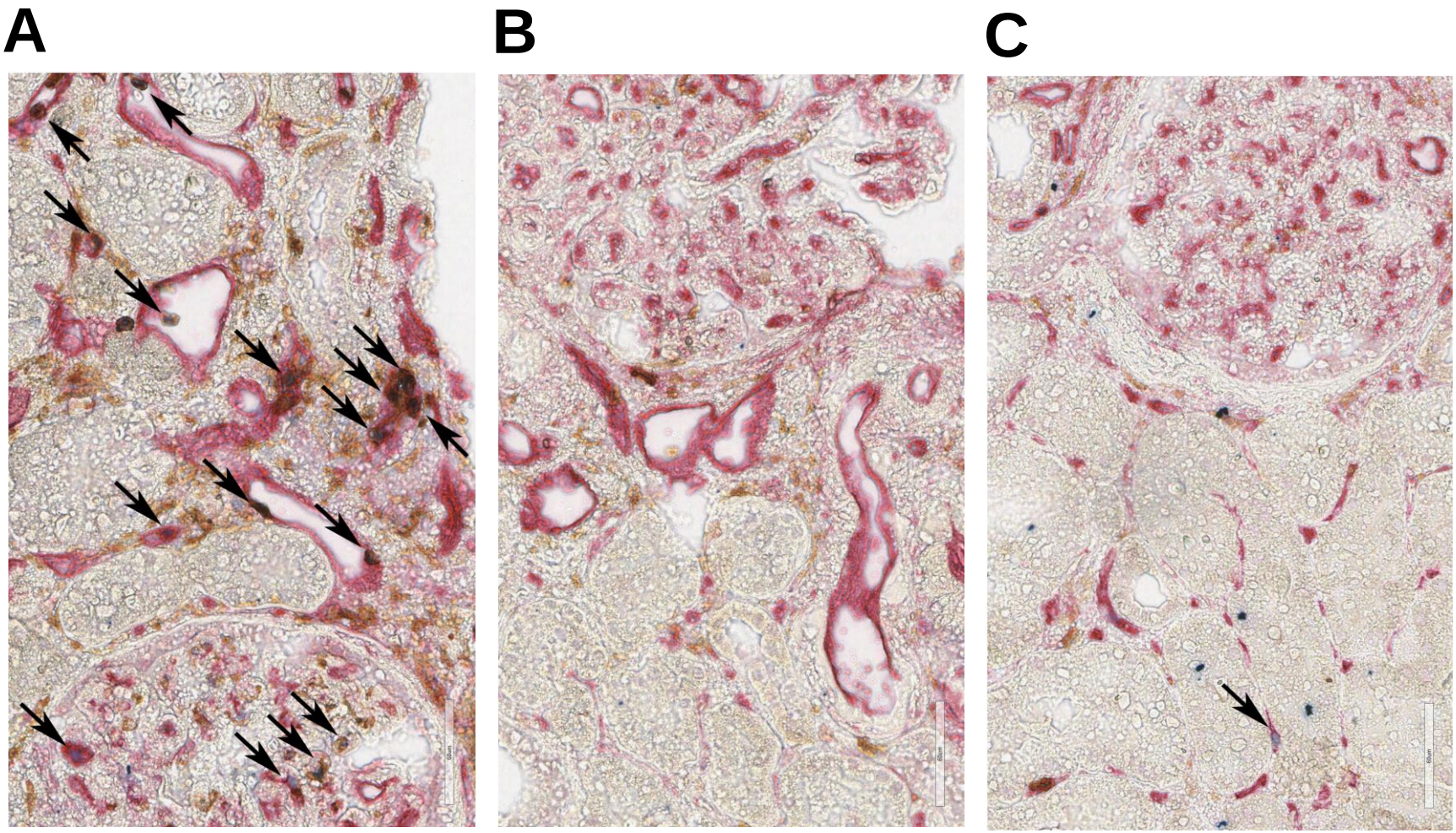

Figure S1. Persistent decrease in intragraft NK cells after daratumumab treatment. (A) Pretreatment biopsy at 400x showing frequent glomerular and peritubular capillary NK cells (arrows), identified by dual CD16 (membrane, brown) and Tbet (nuclear, blue) staining. Endothelial cells are stained with CD34 (red). (B) Biopsy 3 months after initiation of daratumumab treatment showing no NK cells. (C) Biopsy at 9 months showing only rare NK cells. NK cell densities at 0, 3, and 9 months were 14.4, 2.6, and 0.6 cells/mm^2, respectively.

Figure S2

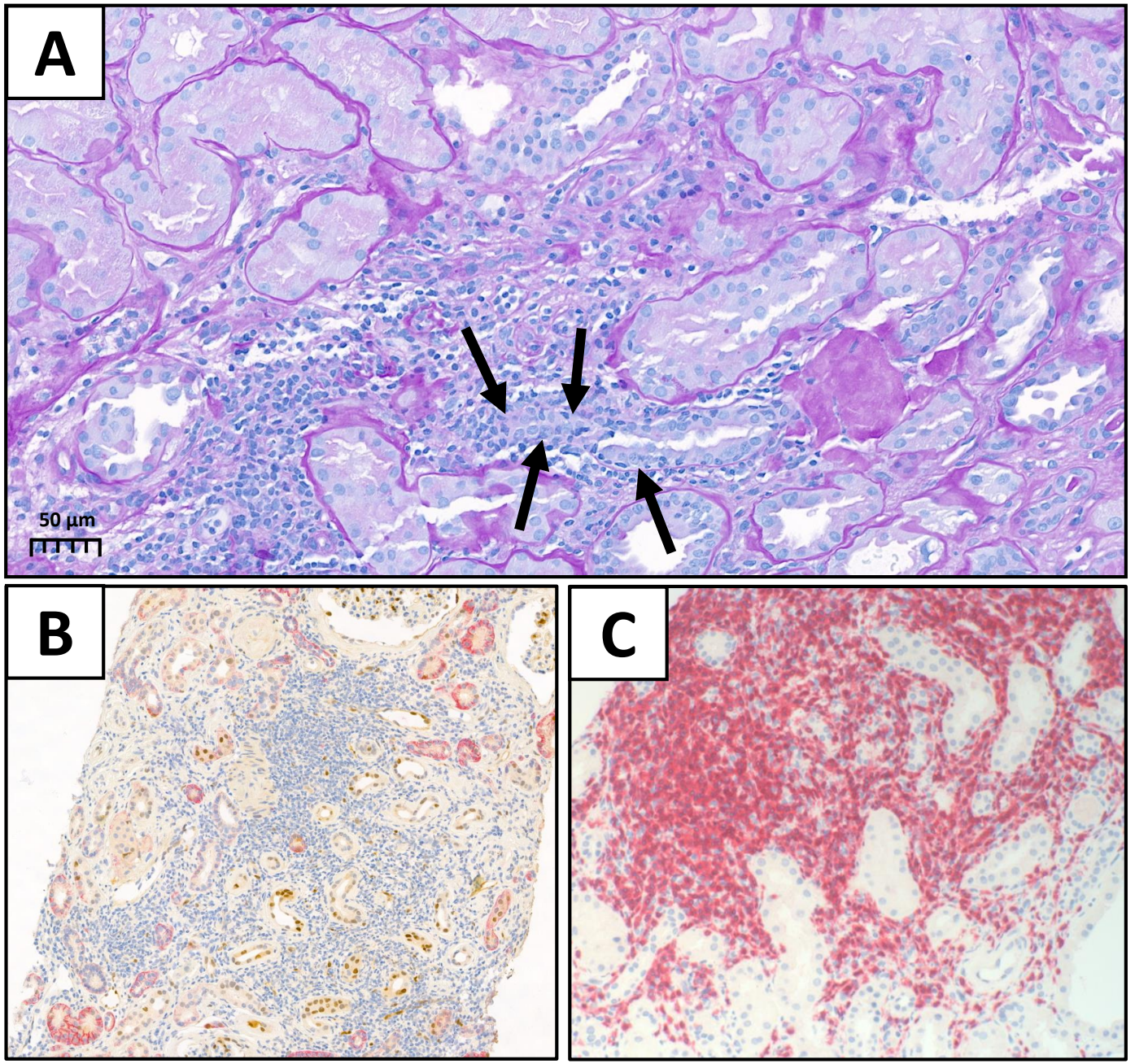

Figure S2. Morphologic and immunohistochemical findings 3 months after initiation of daratumumab treatment. (A) Periodic Acid-Schiff stain illustrating tubulo-interstitial infiltrates. Arrows indicate focal high-grade tubulitis (t3). (B) CD138/bcl-1 staining showing positive CD138 staining (red staining) of tubular epithelial cells but not in the lymphocytic infiltrate [bcl-1: brown staining; nonreactive cells: blue (hematoxylin counterstain)]. (C) CD3 staining (red) showing predominant tubulo-interstitial infiltration by $CD3^+$ cells.

Figure S3

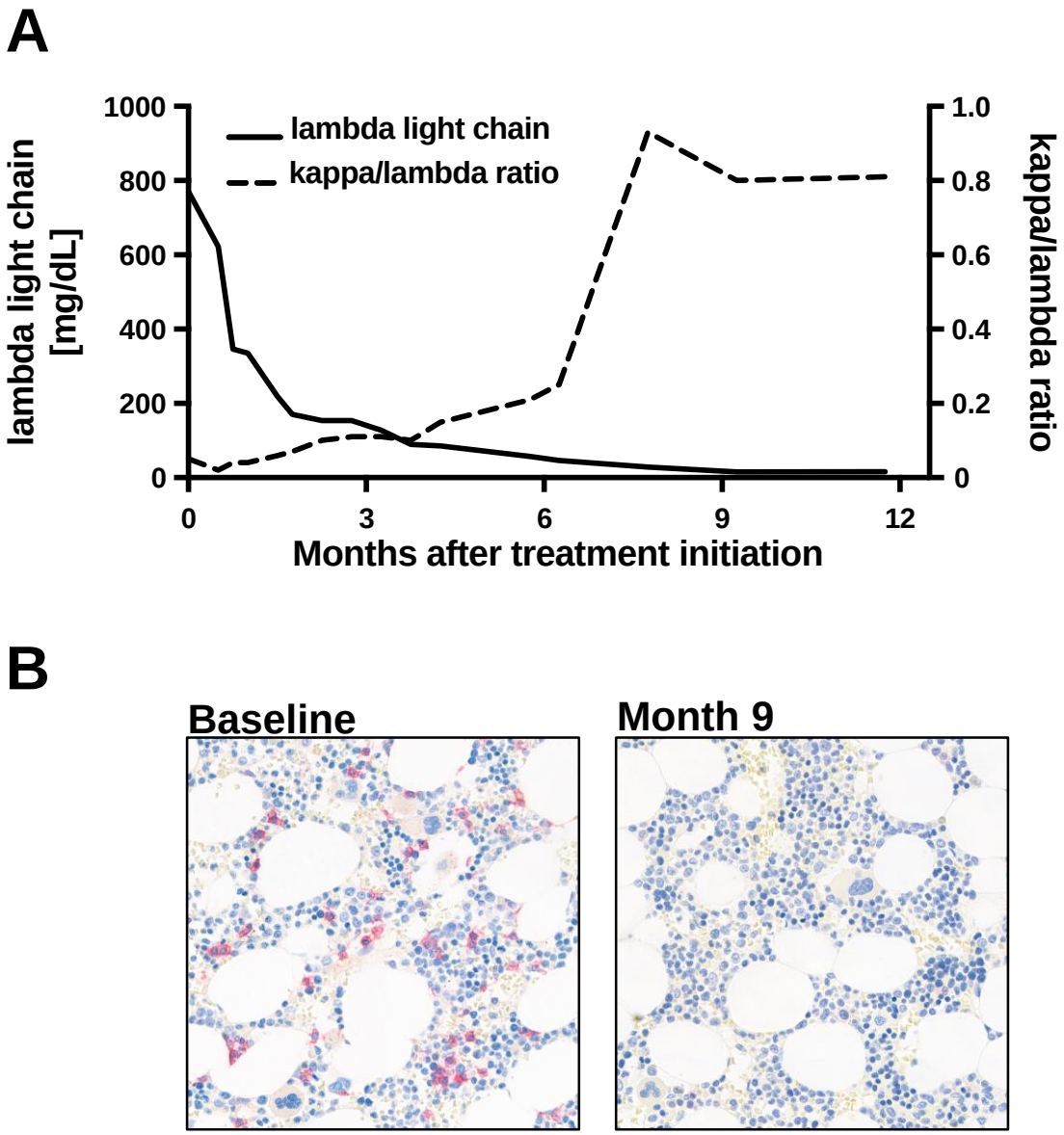
A
lambda light chain
kappa/lambda ratio
lambda light chain [mg/dL]
kappa/lambda ratio
1000
800
600
400
200
0
1.0
0.8
0.6
0.4
0.2
0
0
3
6
9
12
Months after treatment initiation
B
Baseline
Month 9

Figure S3. Impact of daratumumab on light chain levels and the results of bone marrow biopsies. (A) Concentrations of free lambda light chains and the ratio of kappa/lambda light chain levels are shown in relation to daratumumab treatment. Serum free light chains were quantified applying immunonephelometry. (B) Immunohistochemical CD138 staining of bone marrow tissue obtained shortly before and 9 months after treatment (CD38 was not considered for PC definition, because of interference of daratumumab with staining results). At baseline, staining showed multiple $CD138^+$ cells [red staining; blue nuclear staining (counterstain with hematoxylin) indicates nonreactive cells]. At 9 months no $CD138^+$ cells were detectable.

Figure S4

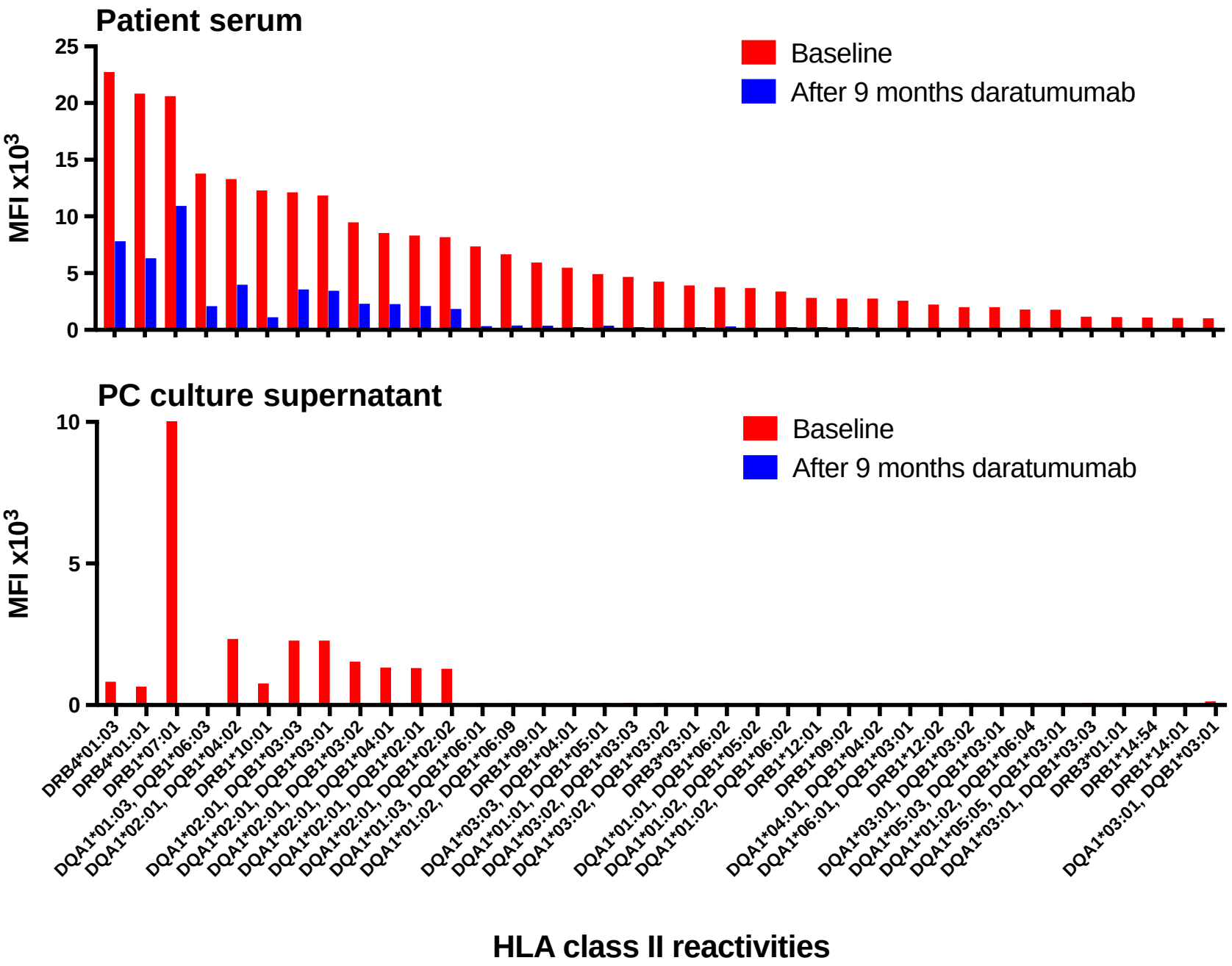
Patient serum
Baseline
After 9 months daratumumab
MFI x10³
25
20
15
10
5
0
PC culture supernatant
Baseline
After 9 months daratumumab
MFI x10³
10
5
0
DRB4*01:03
DRB4*01:01
DRB1*07:01
DQA1*01:03, DQB1*06:03
DQA1*02:01, DQB1*04:02
DRB1*10:01
DQA1*02:01, DQB1*03:03
DQA1*02:01, DQB1*03:01
DQA1*02:01, DQB1*03:02
DQA1*02:01, DQB1*04:01
DQA1*02:01, DQB1*02:01
DQA1*01:03, DQB1*02:02
DQA1*01:02, DQB1*06:01
DRB1*06:09
DRB1*09:01
DQA1*03:03, DQB1*04:01
DQA1*01:01, DQB1*05:01
DQA1*03:02, DQB1*03:03
DQA1*03:02, DQB1*03:02
DRB3*03:01
DQA1*01:01, DQB1*06:02
DQA1*01:02, DQB1*05:02
DQA1*01:02, DQB1*06:02
DRB1*12:01
DRB1*09:02
DQA1*04:01, DQB1*04:02
DQA1*06:01, DQB1*03:01
DRB1*12:02
DQA1*03:01, DQB1*03:02
DQA1*05:03, DQB1*03:01
DQA1*01:02, DQB1*06:04
DQA1*05:05, DQB1*03:01
DQA1*03:01, DQB1*03:03
DRB3*01:01
DRB1*14:54
DRB1*14:01
DQA1*03:01, DQB1*03:01
HLA class II reactivities

Figure S4. Pattern of anti-HLA antibodies in serum and supernatants from bone marrow-derived $CD138^+$ antibody-secreting cells. Panels A and B show the results of single antigen bead arrays (HLA class II panel) for the 37 HLA specificities that were detectable [mean fluorescence intensity (MFI)>1000] in serum at baseline. Antibodies are ordered according to their pretreatment MFI levels in serum, and the respective specificities are listed on the x-axis. Results obtained from serum (A) and supernatants of $CD138^+$ antibody-secreting cells (B) before (red bars) and 9 months after initiation of daratumumab treatment (blue bars) are shown.

Figure S5

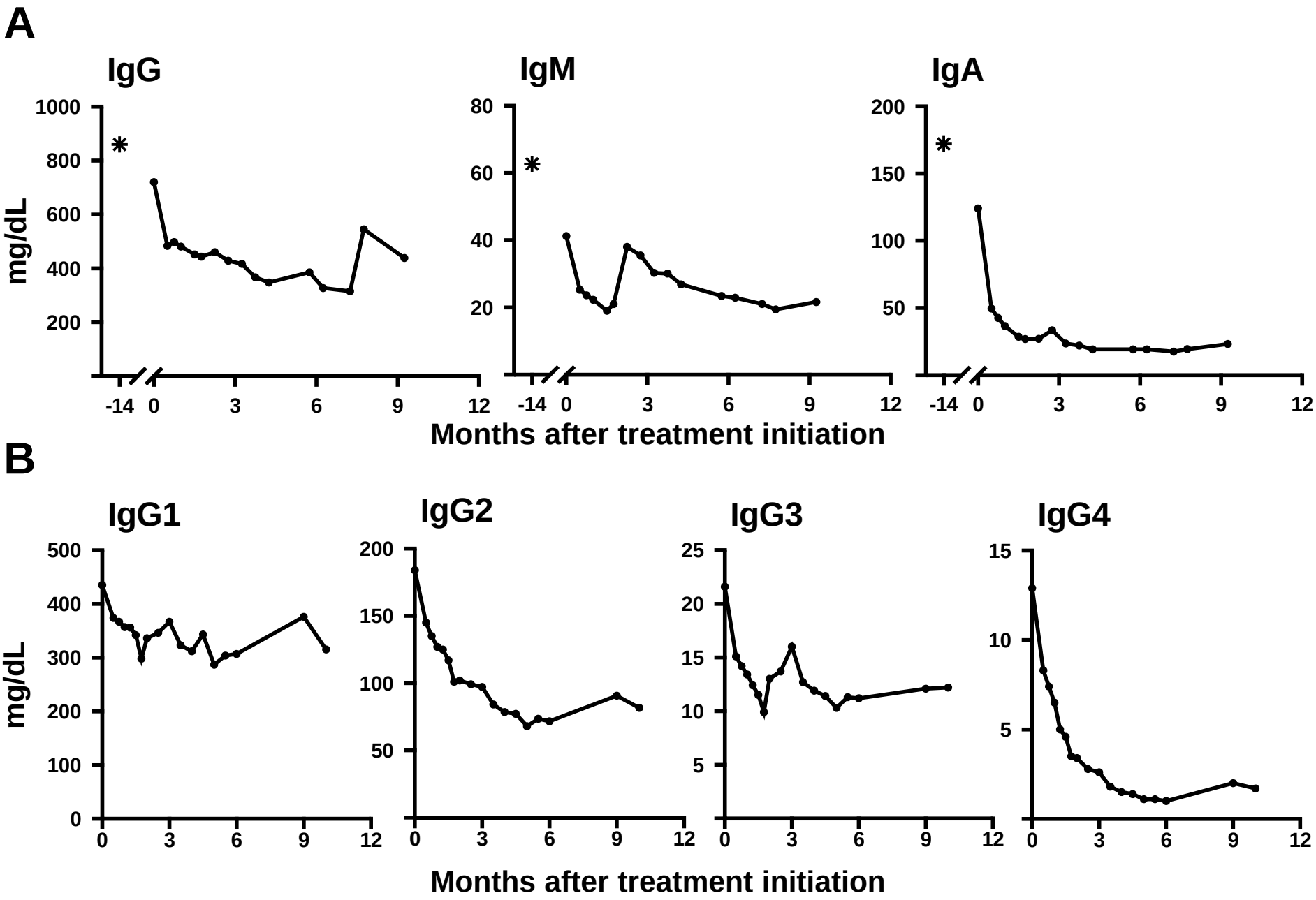
A
IgG
IgM
IgA
mg/dL
1000
800
600
400
200
80
60
40
20
200
150
100
50
-14
0
3
6
9
12
Months after treatment initiation
B
IgG1
IgG2
IgG3
IgG4
mg/dL
500
400
300
200
100
0
200
150
100
50
25
20
15
10
5
15
10
5
0
3
6
9
12
Months after treatment initiation

Figure S5. Impact of daratumumab on immunoglobulin levels. Concentrations of (A) total immunoglobulin (Ig) G, IgM and IgA and (B) IgG1-4 subclasses are shown in relation to daratumumab treatment (baseline = month 0). Total IgG, IgM, IgA, as well as IgG subclasses were quantified from serum applying immunonephelometry. Detection of IgG subclass levels was not part of routine monitoring before treatment initiation.

Figure S6

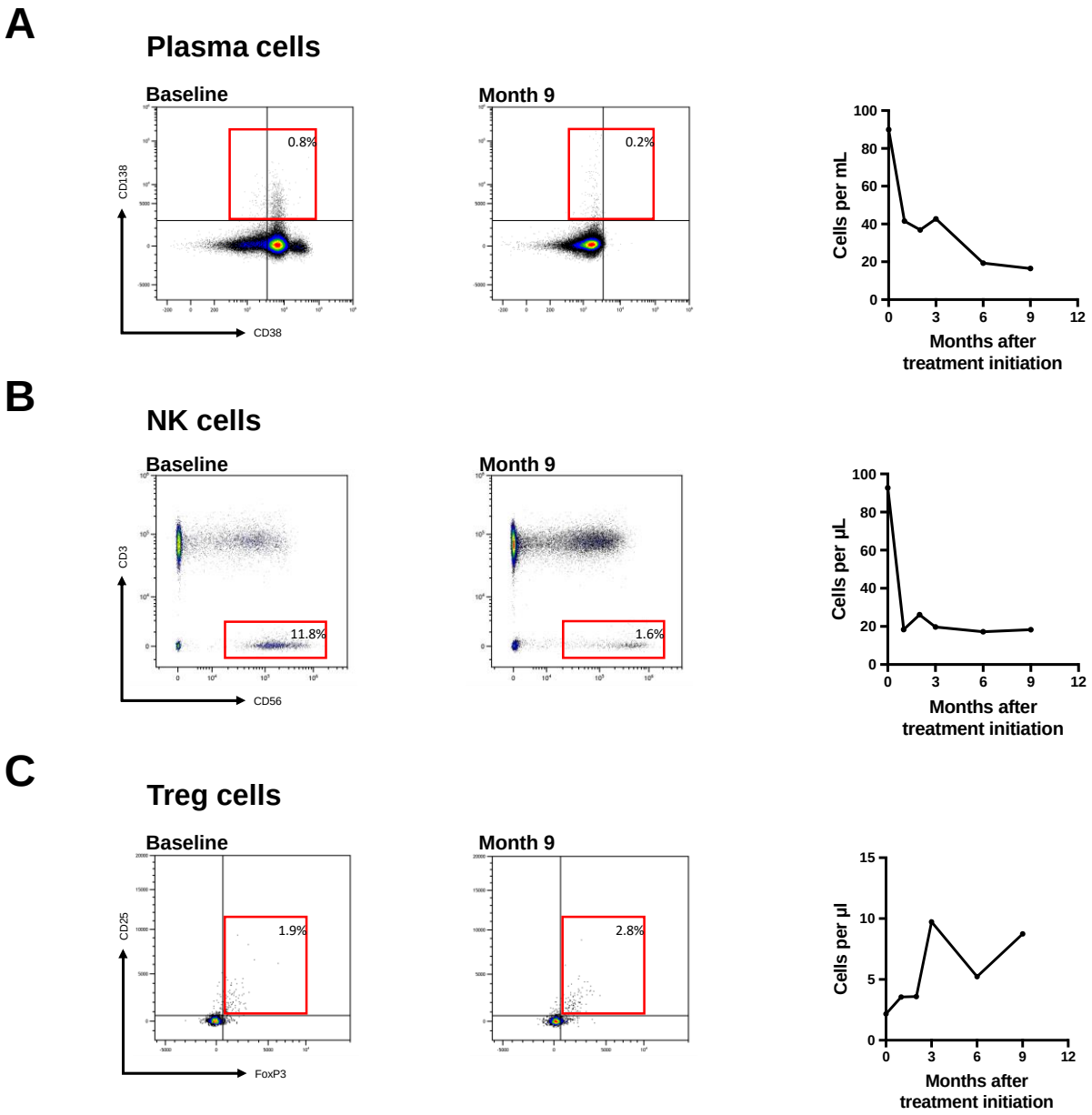
A
Plasma cells
Baseline
0.8%
CD138
CD38
Month 9
0.2%
Cells per mL
Months after treatment initiation
B
NK cells
Baseline
11.8%
CD3
CD56
Month 9
1.6%
Cells per µL
Months after treatment initiation
C
Treg cells
Baseline
1.9%
CD25
FoxP3
Month 9
2.8%
Cells per µl
Months after treatment initiation

Figure S6. Proportions and counts of plasma cells (PC), natural killer (NK) cells and regulatory T cells (Treg) in relation to treatment with daratumumab. For whole blood flow cytometric analysis, standardized preformulated dry antibody panels were applied as described in the methods section. Results are provided as percentages of parent cell populations (pseudocolor plots) as well as absolute counts calculated in relation to white blood cell counts. Plots show the proportions of (A) $CD138^{+}$ PC (after light scatter-based gating on red cell lysed whole blood; CD38 was not considered for PC definition, because of interference of daratumumab with CD38 staining), (B) $CD3^{-}CD56^{+}$ NK cells (after gating for $CD19^{-}$ lymphocytes) and (C) $CD25^{+}FoxP3^{+}$ Treg (after pregating for $CD3^{+}CD4^{+}CD127^{lo}$ T cells within the lymphocyte population), respectively.